Parity-time Symmetric gratings in 1550 nm Distributed-Feedback lasers diodes: insight on device design rules

H. Benisty, Vincent Brac de La Perrière, Abderahim Ramdane, Anatole Lupu

Parity-time Symmetric gratings in 1550 nm Distributed-Feedback lasers diodes: insight on device design rules.

HENRI BENISTY[1,*] VINCENT BRAC,[2] ABDERAHIM RAMDANE,[2] AND ANATOLE LUPU,[2]

[1]*Laboratoire Charles Fabry, Université Paris-Saclay, Institut d'Optique IOGS, 2 Avenue A Fresnel, Palaiseau, France,*
[2]*Center for Nanosciences and Nanotechnologies, Palaiseau, France,*
**henri.benisty@institutoptique.fr*

Abstract: We build up on former results from our work on parity-time symmetric gratings implemented in 1550 nm distributed feedback laser diodes to address the design issues raised by the first observed trends. These laser diodes are of "complex-coupled" nature, with modulations of both real and imaginary part of effective index, with relative phase π/2 related to the parity-time symmetry. The unidirectionality of the photonic behavior in reflection mode is dependent on the level of extra losses incurred by the metallic grating used to implement fixed loss modulation onto a nearly uniform gain, either as a first order or as a third order grating. The observed behavior suggests that facets play a large role in setting the desired "unidirectional" lasing operation points, with preferential emission on one side. We explore this issue, of generic interest for the coupling of parity-time symmetric structures to open space.

1. Introduction

Parity-time symmetry (PTS) has been a remarkably successful concept in optics [1-15]. Blended with periodicity, it naturally introduces an asymmetry or "unidirectionality" in the way dispersion relations are considered [16-18]. The physics and optoelectronics communities have learnt from several pioneers in the last few decades how interesting it was to push periodicity and symmetries to new limits, (notably through metamaterials, active nanophotonics, and chirality, see e.g. Refs. [19-21]). This is basically because a modulation such as the modulation of the complex refractive effective index in a distributed-feedback (DFB) laser diode takes in an ideal limit the simple form $n_{eff}(z) = n_{eff,0} + \delta n \exp(iKz)$, with real part $\delta n \cos(Kz)$ and imaginary part $\delta n \sin(Kz)$ in quadrature, causing a scattering channel only for +K and none for –K, unlike classical real-index grating for instance[22,23].. It must be said that the idea of complex-coupling in DFB gratings was pervasive in the late stage of DFB developments in the 90s [24-31]. Gain modulation at those times was envisioned as stemming from the periodic etching of multi-quantum-well (MQW) stacks [25,27], but the material issues and device performance penalties incurred by such a choice made the outcome not really profitable, and more fundamentally, such strategies set the choice of the relative phase of real and imaginary parts of index to 0 or π, leaving aside the PTS window of opportunity, already envisioned in those years but without the current terminology [31,32].

We recently attempted to implement such PTS DFB lasers diodes [33]. Our aim is to use this fundamental PTS concept and the associated "unidirectional" reflection to address an important issue of real-life telecommunication laser diode systems in fiber networks: the sensitivity of laser coherence to optical feedback, cast as an "ORL" or "optical return loss"[34,35]. If, for some reason along a fiber link, sizable reflections arise, this means return with rather high signal and small "return losses". Such a delayed feedback is well-known to

compromise the laser spectral coherence. As coherent detection is having, since a decade or so, an edge in terms of pushing the bandwidth capability of optical networks to ever-increasing heights (to confront world demand for bandwidth), the attainment of optimal coherence is a prerequisite. The issue is mostly tackled through expensive optical isolators. These devices fundamentally break the transmission matrix reciprocity thanks to magneto-optics. But their cost is a burden on the broader deployment of high-end DFB lasers beyond the core facilities and infrastructures, closer to homes or in the wide and demanding domain of datacom inside data centers (where copper eventually meets its limits at few meters link distances).

Hence, isolator-free solutions are a hallmark of recent device research. Using a fundamental concept to meet this class of goals is our general aim. Our previous work described our first results in that domain. We are going to summarize them briefly in the next section, Sec.2, as the audience is still mostly unaware of this branch of applied research, so as to connect it with the more popular PTS "lab-devices" that have been the center of the focus in the last few years. The issues at stake are the grating order, the loss level, and the impact on spectral purity and on "unidirectionality", as well as the actual impact, in our first tests, on "ORL" level, the key performance, whose values are the subject of regularly updated norms such as IEEE 802.3. In the following, Sec.3, we describe our efforts to understand the combined role of grating characteristics and lasers facets (high or low reflection) in the lasing behavior: since a high-efficiency PTS laser has to operate at moderate level of distributed reflection [36], the way the facets influence the feedback appears as more crucial to our scope than usual. The next section, Sec.4, is specifically devoted to the trends in the role of facets for unidirectionality. We combine the simulation results with our experience from previous work to discuss what an optimal facet design could be in section 5. We then conclude the paper.

2. Experimental findings summary

The InP platform is the reference for 1550 nm telecom laser diode. Few PTS have been investigated on this platform, as it is not the simplest to tailor gain and losses at the wavelength scale. One aspect of good laser diodes is that the active structure is buried, and isolated laterally by epitaxial regrowth of InP of the proper type to channel current from the top electrode to the few-µm-wide MQW active region. The grating generally sits on top of the active layer. A preferred alternative design to access the optical mode's longitudinal landscape periodic modulation is a relatively tall ridge structure, with electrode on top. As show in Fig.1(a), in such a geometry, the MQW is buried just beneath the bottom of the ridge, and the ridge width modulation does translate into a sizable effective index modulation of the laser optical mode, but only of its real part (neglecting radiation losses for third order gratings). Then, as the optical mode still overlaps the bottom region the "cliffs" of the modulated ridge, metal stripes of the same periodicity (or of different periodicity if a different order is chosen) can be implemented on the adjacent area (as done in Ref.[23] for commercial DFB lasers targeting a market of specialty wavelengths), with controlled relative phase.

The essential test of the benefits of PTS systems can then be investigated by tuning the relative phase of the loss and gain parts, Fig.1(b). This amounts to choose the phase ϕ in a general formula of the modulation reading $\delta n(z) = \delta n' \cos(Kz) + i\delta n''\cos(Kz+\phi)$. Of course this phase correspond to a physical shift of the fraction ($\phi/2\pi$) of the grating period $\Lambda = 2\pi/K$ ($\approx m\,\lambda_{laser}/2n_{eff}$ at order $m = 1$ or 3 here).

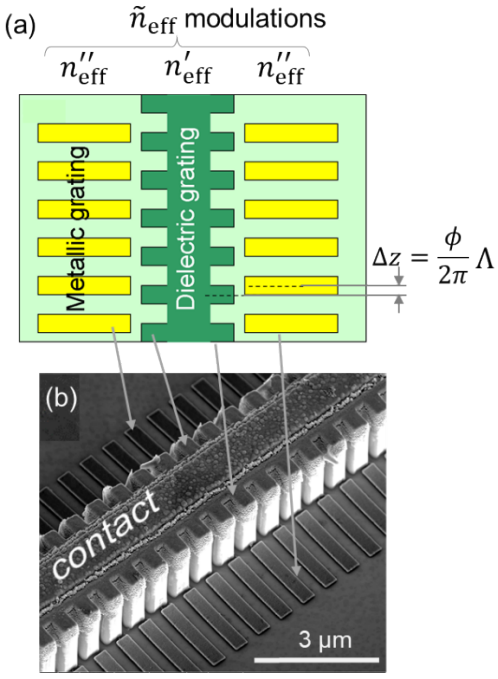

Fig. 1. (a) Sketch of the modulated ridge width that contributes to most of the real index modulation, and of the metallic grating, that is the only contributor the imaginary index modulation. Their relative positions are shifted as indicated. (b) Micrograph (tilted view) of a typical device (3rd order grating, ca. 720 nm pitch) with the dielectric and metallic grating, and the contact on the ridge middle.

The general case is a case of "complex-coupling". In the usual notation, the coupling constant κ is essentially the complex amplitude of δn(z), but here its +K and –K Fourier components should be distinguished: within a factor of 2, they are $\delta n' + i\delta n'' e^{i\phi}$ and $\delta n' + i\delta n'' e^{-i\phi}$, so that the choice $\phi = \pi/2$ and $\delta n' = \delta n'' > 0$ cancels the +K Fourier component of κ and doubles its –K one. From a practical perspective, we have three continuous parameters at hand, the two index modulations and a single phase since we reference the phase to the real part of the grating index modulation (in other words, the four real numbers that control the two Fourier components at K and –K are not independent given the phase reference to the real part of the grating index modulation). Only when it comes to the addition of facets at gratings end points does this reference convention entail some consequences. But for the grating alone it is neutral. A large part of the experimental work was to find the proper technological parameters to get a good laser from this structure, with a reasonably accurate knowledge of the coupling constants (±15%), which was checked by several means. A typical difficulty is that the metal and the optical field overlap most at the critical region of the cliff's foot, where a 30 nm change in metal position, easily found due to the delicate process of defining stripes close to cliffs, has a substantial effect on the inferred (calculated) κ values.

Our study in Ref.[33] compared index-coupled lasers (no metallic grating), gain-coupled lasers (no ridge modulation, only the weaker modulation of real index by the metal survives, but gold at 1550 nm has a small real part of the index), and complex-coupled lasers such as those of Fig.1. However we did not pursue the goal of pure PTS because it would entail metal losses to become excessive. Hence we explored complex-coupled lasers with sizable asymmetries in the κ value seen by the two counter-propagating waves (say 20%), but far from cancelling one with respect to the other. Still, in a laser, small differences in coupling may have large influence on the lasing mode competition.

Spectra with clear single mode behavior and device-grade characteristics in terms of output power (> 5 mW) were observed. Some devices were tested with external sources to check the existing of a substantial anisotropy in reflection in conditions close to transparency. The first ORL tests were also reported in Ref.[33], whereby the coherence collapse was tracked by adequate spectroscopic means under increasing return losses from a desktop-length fiber fitted with a variable loop-based attenuator. An interesting proportion of lasers had sufficient feedback immunity to pass the IEEE802.3 stringent level, one of them tolerating up to –10 dB return. However the data were somehow dispersed and hard to exploit in a clear-cut manner. Fig.2(a) shows for instance that complex-coupled lasers provide very similar spectra on both sides, in spite of the grating asymmetry. For a weak κ value, and henceforth a weak κL value, this is somehow possible, because the two counter-propagating waves are large throughout the device. But it suggests that the extra role of the facets is predominant in these conditions.

A similar conclusion can be drawn from the set of L-I curves from lasers of a same bar, Fig.2(b). These lasers were designs with increasing phases ϕ, by steps of $\pi/4$: this means relative shifts of the dielectric and metallic gratings (Fig.1a) of $\Delta z = \Lambda/8$ ($\Delta z \approx 80$ nm for third-order grating) between the two gratings, from one laser to the adjacent one in the bar. The two PTS lasers manage to get more light on the (conventional) SD side than on the other side denoted SU. But the overall trend is not marked to pinpoint a genuinely major role of PTS-related effects.

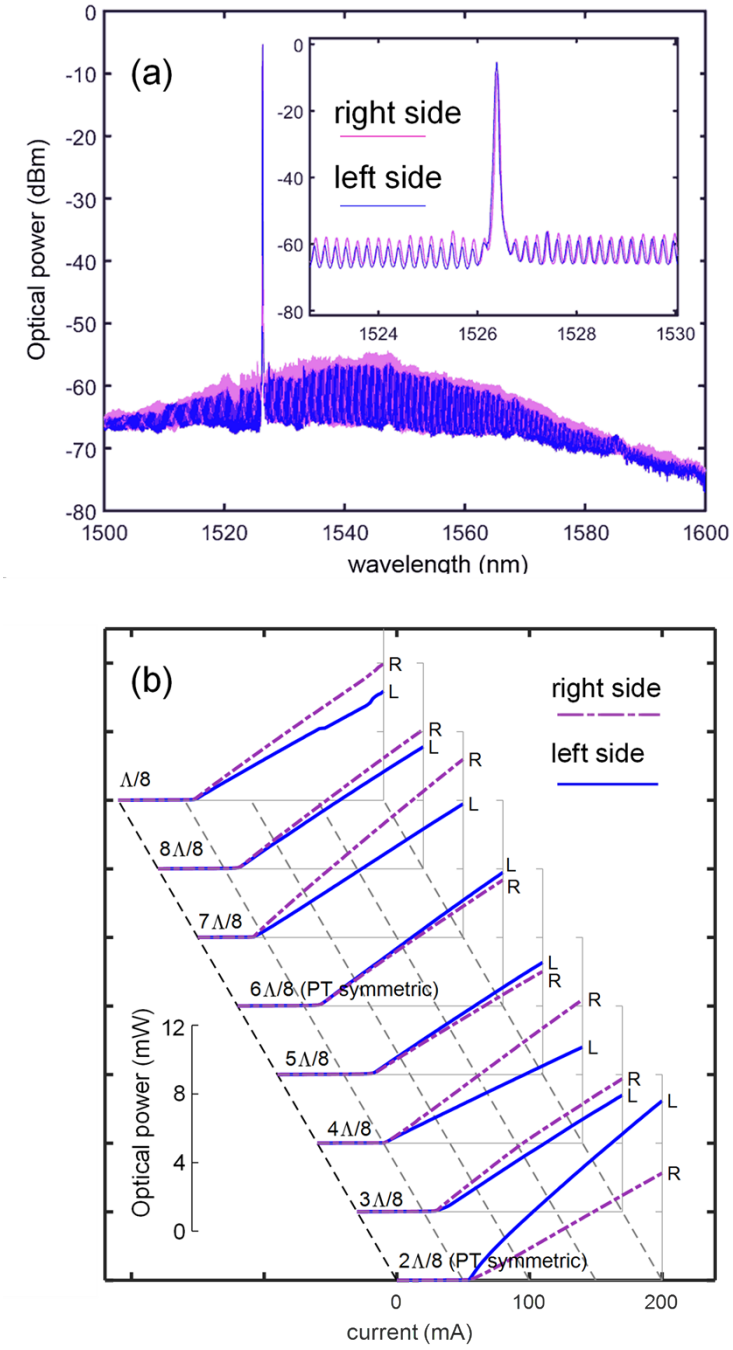

Fig. 2. (a) Typical spectra of a given complex-coupled grating device of length 1960 μm at 200 mA with cleaved facet, taken from both side. The DFB operation does provide single-mode operation and the weak difference shows that this is obtained with a relatively weak κL product (b) L-I data (power vs. intensity) of lasers from the same bar with phases increasing by steps of Λ/8 (equivalently ϕ increasing by steps of π/4); L and R designates the two sides. The data for different phases are shifted along the dashed line. The inner optical power axis (0-12 mW) applies to all data. The L over R preference for the PTS cases is not showing up strongly,

in spite of the existing directionality in reflection [33], with interplay of the laser facets being the likely cause.

In the rest of the paper, we attempt to explain these behaviors by invoking the non-trivial role of the facets in these configurations. The issue is somewhat reminiscent of how the surface cut of metamaterials with underlying periodicity influences the observed properties. The facet reflection (~0.5 in amplitude with antireflection [AR] or high-reflection [HR] coating) is of the same order of magnitude as the single pass reflection from the grating, hence its phase can play a large role.

Such physics already exists for simple DFB index-coupled lasers, but the issue was different: the modal structure of the gain grants two modes with similar gain thresholds on each side of the grating (for first order operation). Then the facets are mainly lifting the degeneracy, and devices are eventually sorted to discard those with unfit SMSR (secondary mode suppression ratio) in terms of acceptable products. Here, we have gratings with a more clearly asymmetric behavior from the start. The facets thus tend to spoil their quality. And we cannot play much the game of quarter-phase shifted DFB with large κL (that naturally grants quite some feedback immunity) because the metal losses would incur a substantial penalty in raising the threshold point. Hence we must clarify the role of facets to assess the viability of our approach in its present form, or inspire solutions that make it good enough for actual devices.

3. Modeling of various gratings and of the impact of variable facets

An important result of the study reported in [20] is that despite the fact that the asymmetry properties of the complex profile grating are spoiled by the reflection of the facets, the combined action of the index- and loss-modulated gratings is nonetheless very beneficial for improving the single-frequency operation of DFB lasers. The reasons for this behavior can be understood by considering the threshold gain required to achieve a lasing emission for the different longitudinal modes inside the DFB laser. This threshold gain can be determined by modeling the DFB laser array as a 1D periodic stack of layers of thickness Λ/8 whose refractive index matches the effective index of the Bragg waveguide at the corresponding position along the light propagation axis. This is illustrated in Fig. 3 on the example of a single grating period of length Λ. Mirrors will be added in the next section, but now the termination are facets with air.

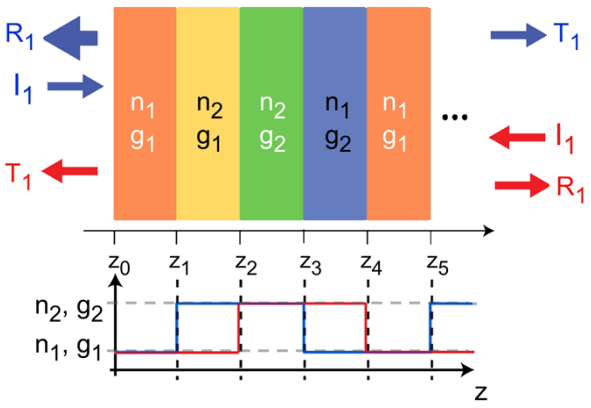

Fig. 3. Schematic of the complex index profile Bragg grating period modeled by the Abelès transmission matrix method.

The relevant longitudinal mode threshold gain g_{th} can classically be determined from the condition of the observation of the first pole of the transmission matrix. To this end we

consider realistic DFB lasers examples with Bragg grating modulation parameters corresponding to those determined from experimental data. We thus revisit classical results but with the extra trends dictated by these values. The distribution as function of wavelength of the transmission poles for 1-mm-long conventional DFB laser with modulation of only real part of the refractive index $\Delta n_{Re} = 0.002$ is shown in Fig. 4a. The two lowest poles at $g_{th} = 32$ dB/cm are corresponding to the onset of a laser emission at the upper and lower edges of the Bragg grating stop-band centered around 1.549 µm. It is obvious that such a dual-frequency operation does not comply with the requirements of telecommunications. Note that the poles located far from the stop band at $g_{th\ FP}$=55 dB/cm are those of the Fabry-Perot cavity, i.e. the wave essentially averaging all grating effects, formed by the end facets with 28% reflection.

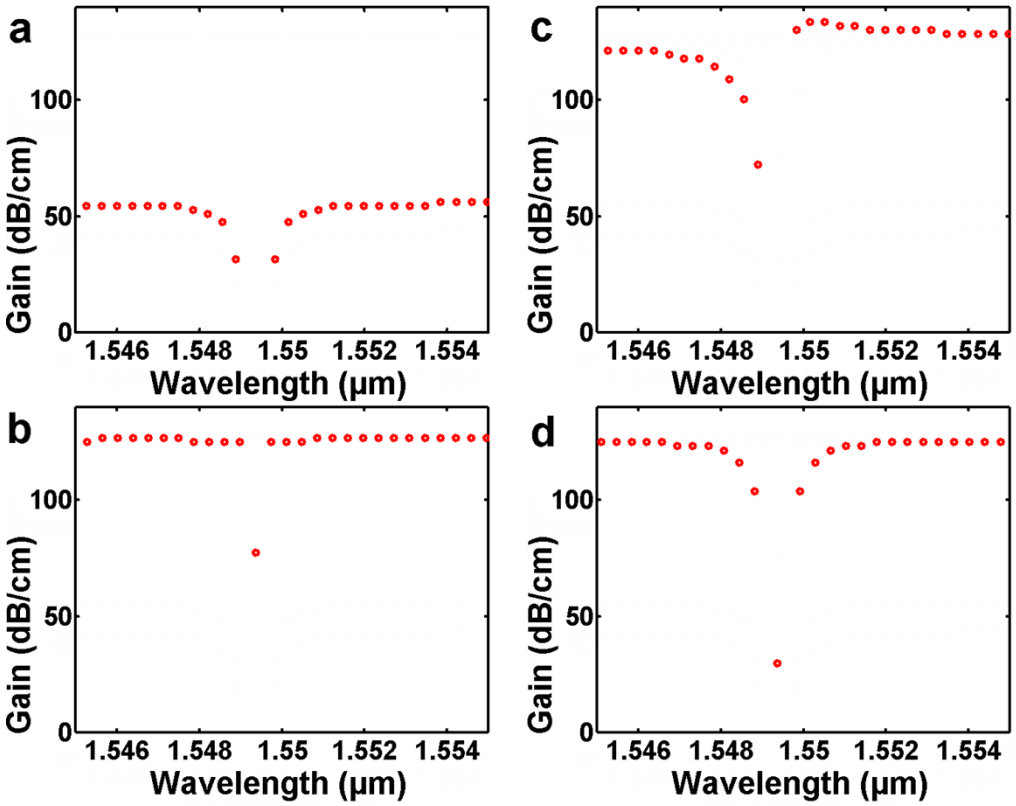

Fig. 4. Maps of the position of the transmission matrix poles for different types of Bragg grating DFB lasers. a) dielectric grating DFB laser with refractive index modulation Δn_{Re}=0.002. b) Metallic grating DFB laser with refractive index modulation Δn_{Im}=0.0004. c) double grating DFB laser with refractive index modulation Δn_{Re}=0.001 and Δn_{Im}=0.0004, φ_{Re}=0, φ_{Im}=π. D) AR and HR coated double grating DFB laser with refractive index modulation Δn_{Re}=0.002 and Δn_{Im}=0.0004, φ_{Re}=0, φ_{Im}=3π/2. R_{AR}=0.079, R_{HR}=0.999.

The case of only loss modulated DFB grating with $\Delta n_{Im} = 0.0004$ is illustrated in Fig. 4b. In contrast to the case of real refractive index modulation, this time a clear single frequency behavior with $g_{th\ Bragg}$=78 dB/cm is observed. The improvement of the single frequency operation is obtained however at the price of an important penalty on the threshold gain. This is also visible from the gain required for reaching Fabry-Perot cavity poles, which is also strongly increased up to $g_{th\ FP}$=122 dB/cm.

The situation corresponding to the complex Bragg grating with $\Delta n_{Re} = 0.002$ and $\Delta n_{Im}=0.0004$ is illustrated in Fig. 4c. The Bragg grating pole level is now $g_{th\ Bragg} = 72$ dB/cm, i.e. 6 dB/cm lower with respect to the case of only loss modulated grating. Note that the gain level of Fabry-Perot cavity poles is the same ($g_{th\ FP} = 122$ dB/cm).

An obvious question is whether it is possible to further reduce the Bragg-grating-related gain-level while keeping single-frequency behavior and high level of gain discrimination with respect to the poles of the Fabry-Perot cavity? The solution to this problem is to use the unidirectional reflection properties characteristic for Parity-Time symmetric gratings. The issue is that in our case on the one hand $\Delta n_{Im} \ll \Delta n_{Re}$, as is clear from the discussion above further increase of Δn_{Im} would be highly detrimental for the threshold gain, and on the other hand, due to the relatively small Bragg grating contrast ($\Delta n_{Re} = 0.002$), the reflection from the grating is strongly spoiled by the facets reflection.

To solve these problems, it is necessary to introduce an additional asymmetry in the system by making one facet highly reflective (HR) and another one with anti-reflection (AR) coating while keeping the relevant product $R_{HR}R_{AR}$ identical to that of an uncoated DFB. When the asymmetry of the facets reflection coincides with that of the Bragg grating (in the sense of favoring stronger reflection on the same side), this results in a strong decrease of the threshold gain. The corresponding situation is illustrated in Fig. 4d with a less-demanding value $R_{AR} = 0.08$. As can be seen, $g_{th\ Bragg}$ is reduced down to 30 dB/cm and this pole is separated by at least 70 dB/cm from the nearest poles.

This result implies very stable single-frequency operation of the DFB laser, but it was obtained for a particular example of a 1-mm-long DFB laser with an *integer number* of grating periods. This choice could be far from neutral, as the interplay of facet reflectivity and grating reflectivity is strong, both having similar orders of magnitude. However, in practice, it would be very difficult to control the exact grating termination with the corresponding precision of $\lambda/30$. Therefore, it is important to evaluate the robustness of single-frequency operation compared to random phase termination of the ends of AR and HR coated Bragg gratings.

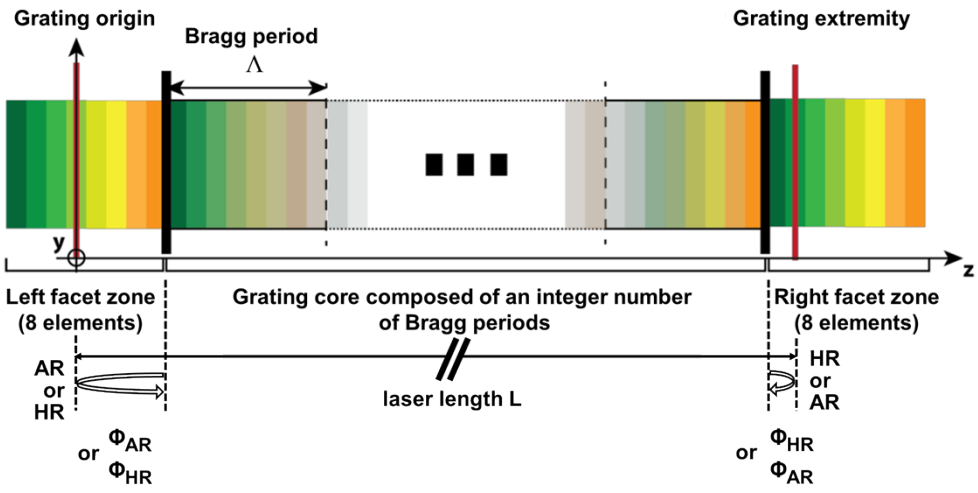

Fig. 5. Schematic of the complex index profile Bragg grating modeled by the transmission matrix method. The phases of the two facets (AR and HR) are scanned throughout the 1-period long outer zones, and the study is carried out for either AR/HR and HR/AR choices, given the PTS grating asymmetry. The period is much smaller than the length ($\Lambda \ll L$).

This can be done by introducing the facet termination related phase defined as the ratio of the incomplete terminal period of length L with respect to the Bragg period Λ (see Fig. 5), then determining the lowest $g_{th\ Bragg}$ in the spectrum for each pair of values of AR and HR facet phases. The results of such a procedure are shown in Fig 6.

In the case when the grating asymmetry coincides with that of complex Bragg grating (AR and obviously laser output on the low reflection side of the grating), there are large white color regions visible in Fig. 6a corresponding to the relatively low threshold gain $g_{th\ Bragg} < 40$ dB/cm. The remarkable feature is that these regions are rather weakly sensitive to the exact phase (position) of the AR-coated end facet termination. In contrast, they are confined to specific areas of the HR coated end facet termination, namely phases around ±45° or ±50°. The total yield corresponding to the white colored regions can therefore be estimated to at least 25% for a fabrication with a random facet phase.

The situation is very different in the case when the asymmetry of AR and HR facets reflection is opposite with respect to that of the Bragg grating. This can be understood physically, as the wave amplitudes are not fitting those of the Bloch eigenmodes of the grating on account of the HR reflection in particular when the local mode would seek low reflection. The unidirectional properties similar to those of loss-modulated Bragg grating are thus showing up, despite the fact that the modulation of the imaginary part of index profile $\Delta n_{Im} = 0.0004$ is five times lower with respect to the modulation of the real part $\Delta n_{Re} = 0.002$. Hence, the interplay of facets and gratings cannot be devised in “rather additive” terms. But fortunately, the good solution still offers a tractable landscape allowing for random facet fabrication with acceptable yields.

In addition to the low threshold gain level, AR/HR coated lasers also exhibit a high level of gain discrimination between the lowest and next pole. The corresponding situation is shown in Fig. 6b. These results ensure a stable single-frequency lasing with a high SMRS level and also provide the expectation of a better tolerance with respect to optical return loss.

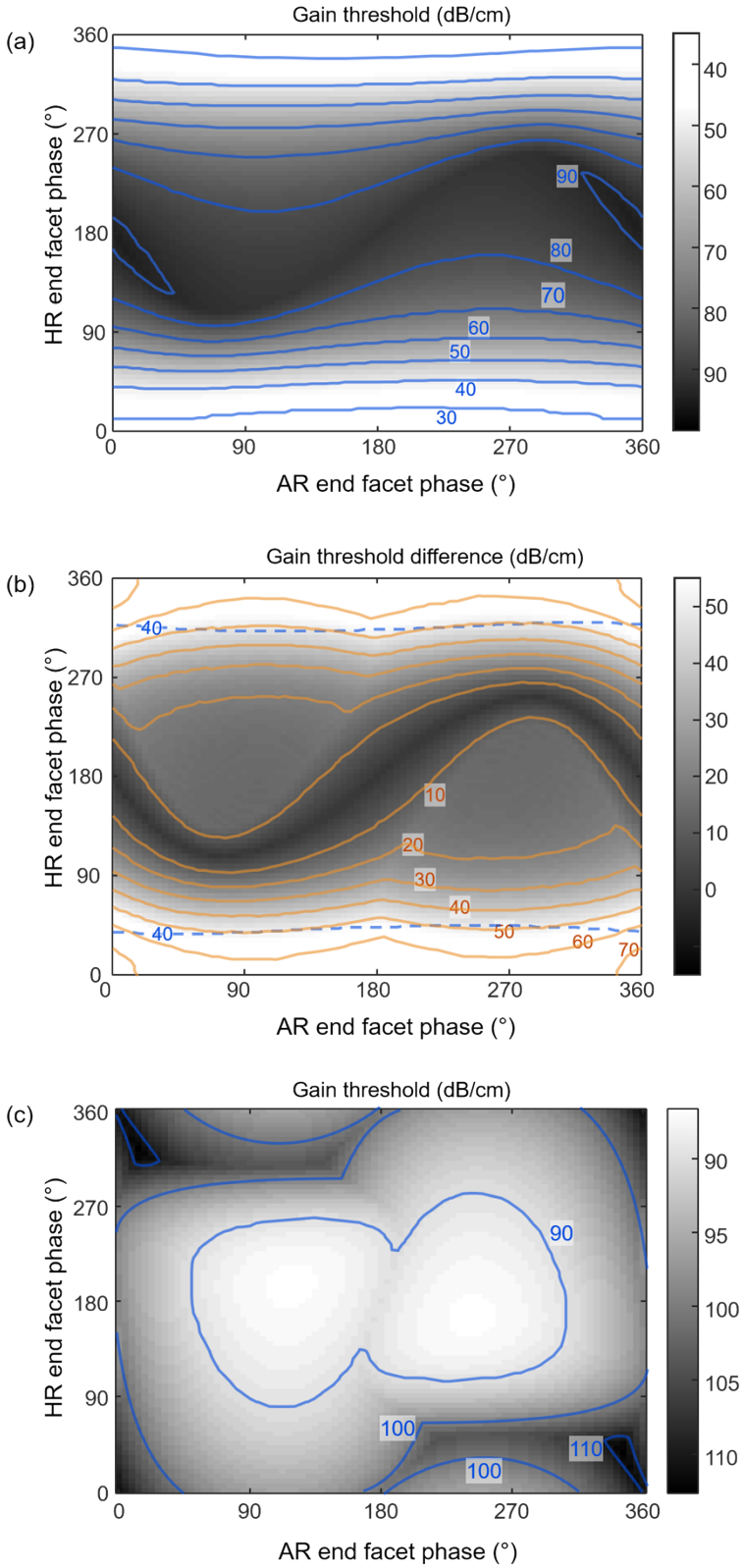
(a)
Gain threshold (dB/cm)
HR end facet phase (°)
AR end facet phase (°)
0
90
180
270
360
90
80
70
60
50
40
30
40
50
60
70
80
90
(b)
Gain threshold difference (dB/cm)
HR end facet phase (°)
AR end facet phase (°)
40
10
20
30
40
50
60
70
40
50
40
30
20
10
0
(c)
Gain threshold (dB/cm)
HR end facet phase (°)
AR end facet phase (°)
90
100
110
100
90
95
100
105
110

Fig. 6. Color maps showing variation of the threshold gain $g_{th\,Bragg}$ and threshold gain difference as a function of both the AR and the HR facets phase, when the asymmetry of AR and HR coatings reflectivity coincides with that of complex profile Bragg grating (HR on high reflective side of grating). (a) Gain threshold map with contours. Note the weak dependence on the AR facet for the low-threshold regime of HR phase around 0°/360° (for the opposite choice, AR and HR anti-coinciding, the gain threshold map is mostly above 85 dB/cm). (b) Map of the gain difference with their contours. The dashed line is the 40 dB gain-threshold contour of (a), delimiting the low threshold area. The secondary mode suppression ratio (SMSR) seems also good in those areas, essentially above 50 dB; (c) Gain threshold map in the case when the asymmetry of the PTS Bragg grating reflection is opposite to the asymmetry of AR/HR coating.

4. Conclusion

Laser diode with PTS symmetry in the DFB grating generalize the constrained complex-coupled DFB laser diodes that was first explored across the 90s. Continued interest for broader operating characteristics of real-life DFB lasers in networks of all kinds is a logical incentive to explore novel solutions such as PTS DFB laser diodes. We have specifically explored the role of grating cut by randomly placed facets in the non-trivial complex-coupled distributed-feedback lasers, based on our previous first experimental results. The interplay of facet and gratings was expected due to the order of magnitude of the reflection and the coherent nature of the interaction, but its physics was not hitherto reported. The issue bears some similarity with the generic issues of cutting into complex metamaterial with elaborate unit cells. We found relevant trends from an adapted version of the classical transmission matrix tool and threshold gain analysis.

The main result here is that a choice of relatively well mastered HR and AR facets can be put to good use to get low-threshold devices with a decent yield (>50%), with only a penalty of the HR facet position. A low threshold of about 32 dB/cm modal gain is predicted for 1-mm-long PTS DFB laser diode devices having our measured real and complex grating modulation characteristics with only one fifth of complex modulation. A more complete study of SMSR and immunity to optical feedback should help defining optimal devices. With the trend found here and the rather clear physical basis for their understanding, the desired properties of large SMSR and strong immunity could see their emergence largely favored.

Acknowledgments

This work has partially been funded by the by the French Agence Nationale pour la Recherche (project “PARTISYMO”, contract number N° ANR-18-CE24-0024-01), and partly supported by the French RENATECH network. We are very grateful to Q. Gaimard, G. Aubin, S. Guilet, L. Le Gratiet, K. Merghem, F. Raineri and C. Ulysse for their expert help in many ways. VB acknowledges financial support from EDOM “Ecole Doctorale” through a PhD grant.

References

1. C. M. Bender, and S. Boettcher, "Real spectra in non-Hermitian Hamiltonians having PT symmetry," Phys. Rev. Lett. **80**(24), 5243-5246 (1998).
2. C .E. Rüter, K. G. Makris, R. El-Ganainy, D. N. Christodoulides, M. Segev, and D. Kip, "Observation of parity–time symmetry in optics," Nature Physics **6**(3), 192-195 (2010).
3. R. El-Ganainy, K. G. Makris, D. N. Christodoulides, and Z. H. Musslimani, “Theory of coupled optical PT-symmetric structures,” Opt. Lett. **32**(17), 2632-2634 (2007).
4. K. G. Makris, R. El-Ganainy, D. N. Christodoulides, and Z. H. Musslimani, “Beam dynamics in PT symmetric optical lattices,” Phys. Rev. Lett. **100**(10), 103904 (2008).
5. Z. H. Musslimani, K. G. Makris, R. El-Ganainy, and D. N. Christodoulides, “Optical solitons in PT periodic potentials,” Phys. Rev. Lett. **100**(3), 030402 (2008).

6. A. Guo, G. J. Salamo, D. Duchesne, R. Morandotti, M. Volatier-Ravat, V. Aimez, G. A. Siviloglou, and D. N. Christodoulides, “Observation of PT-Symmetry Breaking in Complex Optical Potentials,” Phys. Rev. Lett. **103**(9), 093902 (2009).
7. S. Longhi, “PT-symmetric laser absorber,” Phys. Rev. A **82**(3), 031801 (2010).
8. Y. D. Chong, L. Ge, and A. D. Stone, “Coherent perfect absorbers: time-reversed lasers,” Phys. Rev. Lett. 106, 093902 (2011).
9. L. Feng, Z. J. Wong, R.-M. Ma, Y. Wang, and X. Zhang, “Single-mode laser byparity-time symmetry breaking,” Science **346**(6212), 972-975 (2014).
10. H. Hodaei, M.A. Miri, M. Heinrich, D. N. Christodoulides, and M. Khajavikhan, “Parity-time-symmetric microring lasers,” Science **346**(6212), 975-978 (2014).
11. B. Peng, S. K. Özdemir, S. Rotter, H. Yilmaz, M. Liertzer, F. Monifi, C. M. Bender, F. Nori, and L. Yang, “Loss-induced suppression and revival of lasing,” Science **346**(6207), 328-332 (2014).
12. L. Feng, Y.-L. Xu, W. S. Fegadolli, M.-H. Lu, J. E. B. Oliveira, V. R. Almeida, Y.-F. Chen, and A. Scherer, “Experimental demonstration of a unidirectional reflectionless parity-time metamaterial at optical frequencies,” Nat. Mater. **12**(2), 108-113 (2012).
13. MA Miri, P LiKamWa, DN Christodoulides, “Large area single-mode parity–timesymmetric laser amplifiers”, Optics letters **37**, 764-766 (2012).
14. H. Hodaei, M.-A. Miri, M. Heinrich, D. N. Christodoulides, and M. Khajavikhan, “PTsymmetric large area single mode DFB lasers,” in Proceedings of CLEO: 2014 (OSA, 2014), Vol. 1, paper FM1D.3.
15. J. Gu, X. Xi, J. Ma, Z. Yu, and X. Sun, X. “Parity–time-symmetric circular Bragg lasers: a proposal and analysis. Scientific reports,” **6**(1), 1-7 (2016).
16. M. Kulishov, J. M. Laniel, N. Bélanger, J. Azaña, and D. V. Plant, "Nonreciprocal waveguide Bragg gratings," Opt. Express **13**(8), 3068-3078 (2005).
17. Z. Lin, H. Ramezani, T. Eichelkraut, T. Kottos, H. Cao, H., and D. N. Christodoulides, "Unidirectional invisibility induced by P T-symmetric periodic structures," Phys. Rev. Lett. **106**(21), 213901 (2011).
18. D. Jalas, A. Petrov, M. Eich, W. Freude, S. Fan, Z. Yu, R. Baets, M. Popović, A. Melloni,J. D. Joannopoulos, M. Vanwolleghem, C. Doerr, and H. Renner, "What is—and what is not—an optical isolator," Nature Photonics **7**(8), 579-582 (2013).
19. S. Droulias, I. Katsantonis, M. Kafesaki, C.M. Soukoulis and E. Economou, "Chiral Metamaterials with PT Symmetry and Beyond,” Phys. Rev. Lett. **122**(21), 213201 (2019).
20. I. D’Amico, D. G. Angelakis, F. Bussières, H. Caglayan, C. Couteau, T. Durt, B. Kolaric, P. Maletinsky, W. Pfeiffer, P. Rabl, A. Xuereb, and M. Agio, "Nanoscale quantum optics," Riv. Nuovo Cim. **42**(4), 153–195 (2019).
21. R. Zhao, T. Koschny, and C. M. Soukoulis, "Chiral metamaterials: retrieval of the effective parameters with and without substrate," Opt. Express **18,** 14553-14567 (2010).
22. A. Yariv, and M. Nakamura, "Periodic structures for integrated optics," IEEE J. Quantum Electron. **13**(4), 233-253 (1977).
23. C. T. Santis, S. T. Steger, Y. Vilenchik, A. Vasilyev, and A. Yariv, "High-coherence semiconductor lasers based on integral high-Q resonators in hybrid Si/III-V platforms," Proc. Nat. Acad. Sci. **111**(8), 2879-2884 (2014).
24. S. T. Kim, and B. G. Kim, "Analysis of single-mode yields above threshold for complex-coupled distributed feedback lasers with asymmetric facet reflectivities," J. Opt. Soc. Am. B **22**(5), 1010-1015 (2005).
25. A. Champagne, R. Maciejko, D. M. Adams, G. Pakulski, B. Takasaki, and T. Makino, "Global and local effects in gain-coupled multiple-quantum-well DFB lasers," IEEE J. Quantum Electron. **35**(10), 1390-1401 (1999).
26. R. G. Baets, K. David, and G. Morthier, "On the distinctive features of gain coupled DFB lasers and DFB lasers with second-order grating," IEEE J. Quantum Electron. **29**(6), 1792-1798 (1993).
27. Y.Luo, Y. Nakano, K. Tada, T. Inoue, H. Hosomatsu, and H. Iwaoka, "Purely gain-coupled distributed feedback semiconductor lasers," Appl. Phys. Lett. **56**(17), 1620-1622 (1990).
28. E. Kapon, A. Hardy, and A. Katzir, "The effect of complex coupling coefficients on distributed feedback lasers," IEEE J. Quantum Electron. **18**(1), 66-71 (1982).
29. G. Morthier, P. Vankwikelberge, K. David, and R. Baets, "Improved performance of AR-coated DFB lasers by the introduction of gain coupling," IEEE Photon. Technol. Lett. **2**(3), 170-172 (1990).
30. D.A. Cardimona, M. P., Sharma, V., Kovanis, and A. Gavrielides, "Dephased index and gain coupling in distributed feedback lasers," IEEE J. Quantum Electron. **31**(1), 60-66 (1995).
31. Y. Boucher, O. Dellea, and J. Le Bihan, "Quasi-periodic complex-coupled distributed-feedback structures with an exponential-like gradient of coupling," IEEE J. Quantum Electron. **33**(12), 2137-2145 (1997).
32. Y. Boucher, "Non-reciprocal effects of complex-coupled distributed-feedback structures resulting from the phase difference between the coupling constants," Optics Commun. **136**(5-6), 410-414 (1997).
33. V. Brac de la Perrière, Q. Gaimard, H. Benisty, A. Ramdane, and A. Lupu, "Electrically injected parity-time symmetric distributed feedback laser diodes (DFB) for telecom applications" Nanophotonics **10**(4), 1309-1317 (2021).
34. S. Azouigui, B. Dagens, F. Lelarge J.-G. Provost, D. Make, O. Le Gouezigou, A. Accard, A. Martinez, K. Merghem, F. Grillot, O. Dehaese, R. Piron, S. Loualiche, Q. Zou, and A. Ramdane, "Optical feedback tolerance of quantum dot and quantum dash based semiconductor lasers operating at 1.55 μm," IEEE J. Sel. Top. Quantum Electron. **15**(3), 764-773 (2009).

35. C. Ke, X. Li, and Y. Xi, "Parity-time symmetric complex-coupled distributed feedback laser with excellent immunity to external optical feedback," AIP Advances **7**(3), 035010 (2017).
36. K. David, G. Morthier, P. Vankwikelberge, R. G. Baets, T. Wolf, and B. Borchert, “Gain-coupled DFB lasers versus index-coupled and phase shifted DFB lasers: a comparison based on spatial hole burning corrected yield,” IEEE J. Quantum Electron. **27**(6), 1714-1723 (1991).
37. J. Seufert, M. Fischer, M. Legge, J. Koeth, R. Werner, M. Kamp, and A. Forchel, "DFB laser diodes in the wavelength range from 760 nm to 2.5 μm," Spectrochim. Acta A Mol. Biomol. Spectrosc. **60**(14), 3243-3247 (2004).